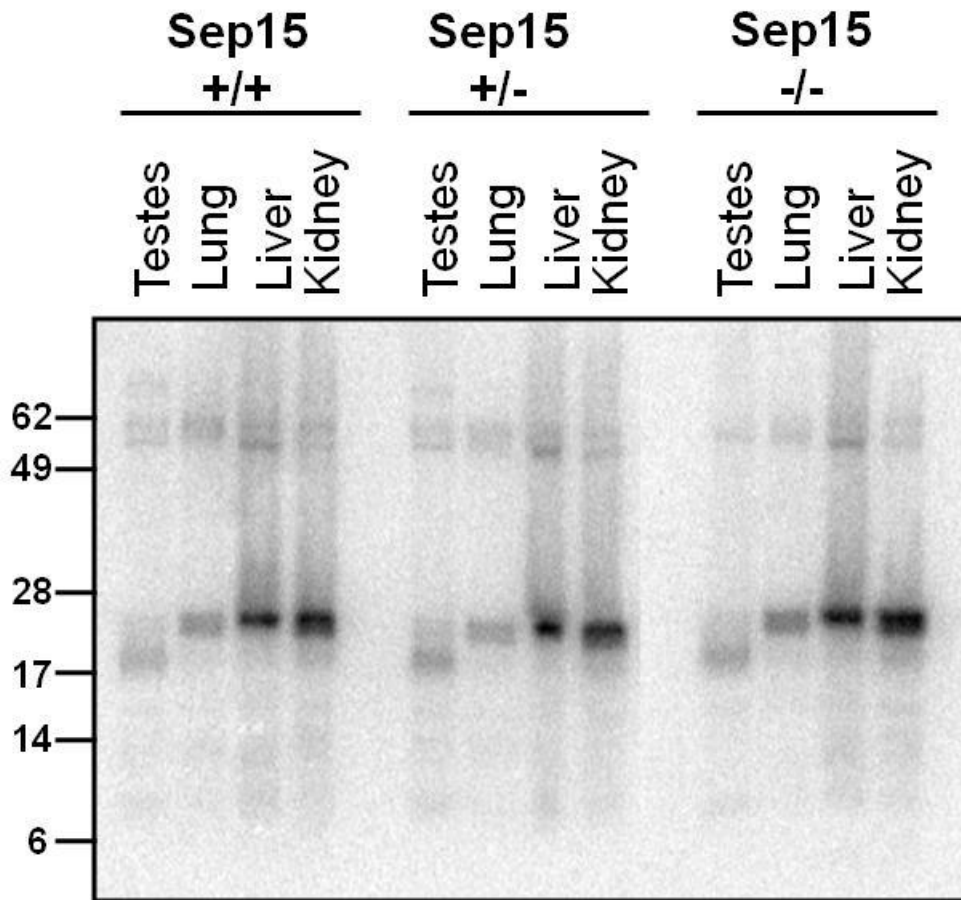
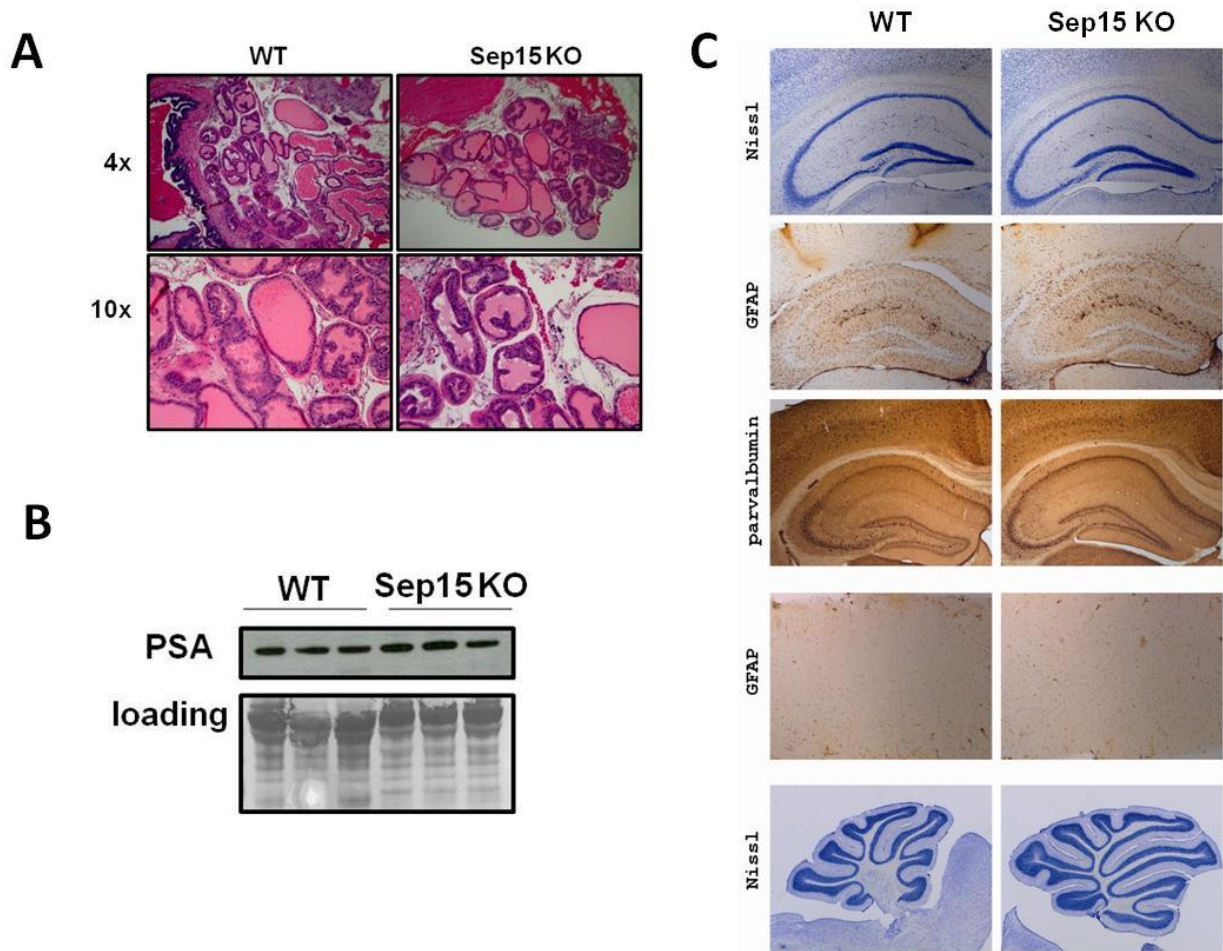


Supplementary information



**Figure S1. Metabolic labeling of WT and Sep15 KO mice with  $^{75}\text{Se}$ .** WT (Sep15<sup>+/+</sup>), and heterozygous (Sep15<sup>+/-</sup>) and homozygous (Sep15<sup>-/-</sup>) Sep15 KO mice were each injected with 40  $\mu\text{Ci}$  of  $^{75}\text{Se}$ . Selenoprotein expression was analyzed in indicated organs by SDS-PAGE followed by PhosphorImager.



**Figure S2. Analysis of prostate and brain pathologies in Sep15 KO mice.** (A) H&E staining of prostate sections in WT and Sep15 KO mice. (B) Western blot analysis of PSA in serum of WT and Sep15 KO mice (upper panel). Coomassie Blue staining as a protein loading control (loading). (C) Analysis of brain sections: Nissl, GFAP and parvalbumin staining of the hippocampal area of WT and Sep15 KO mice. Also shown are immunohistochemistry of cerebral cortex area with GFAP antibodies and Nissl staining of cerebellum.

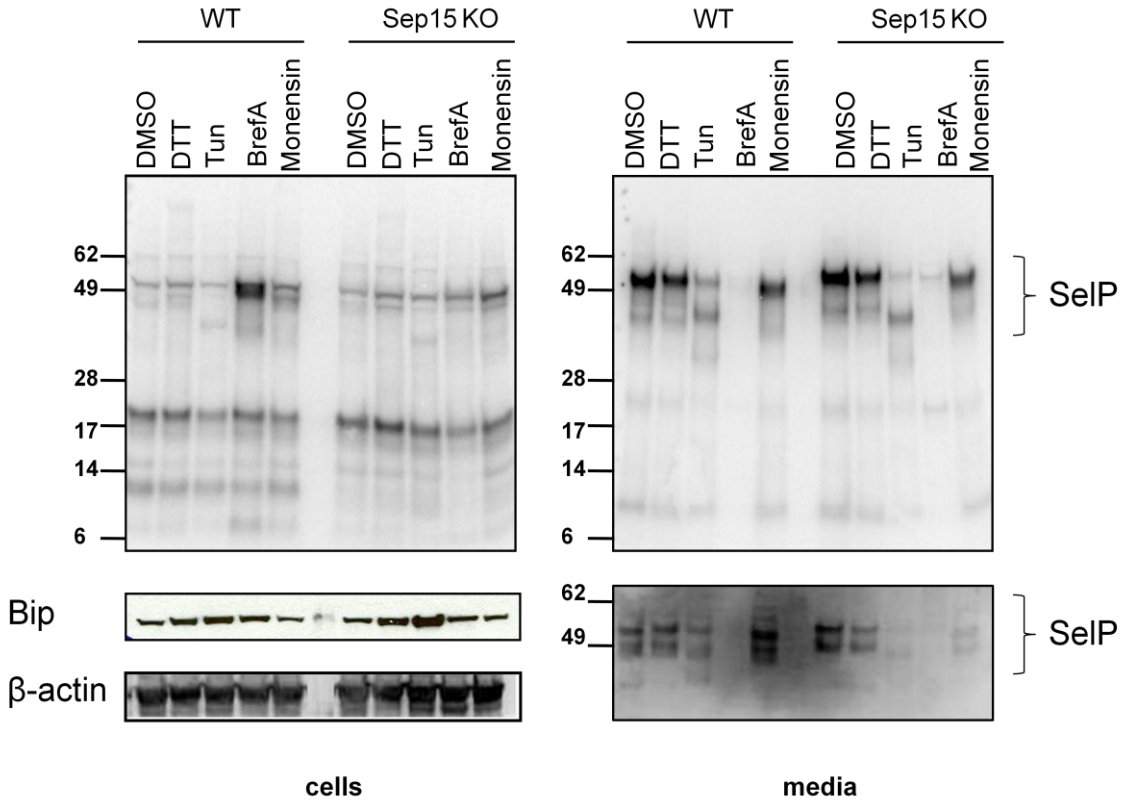


**Figure S3. Sep15 deficiency does not affect SeIP secretion.** Hepatocytes were isolated from WT and Sep15 KO mice and metabolically labeled with  $^{75}\text{Se}$ . PhosphorImager analysis of cellular extracts (left panel) and concentrated media (right panel). Membranes were further analyzed with BiP and  $\beta$ -actin (lower left panels) and SeIP (lower right panel) antibodies.

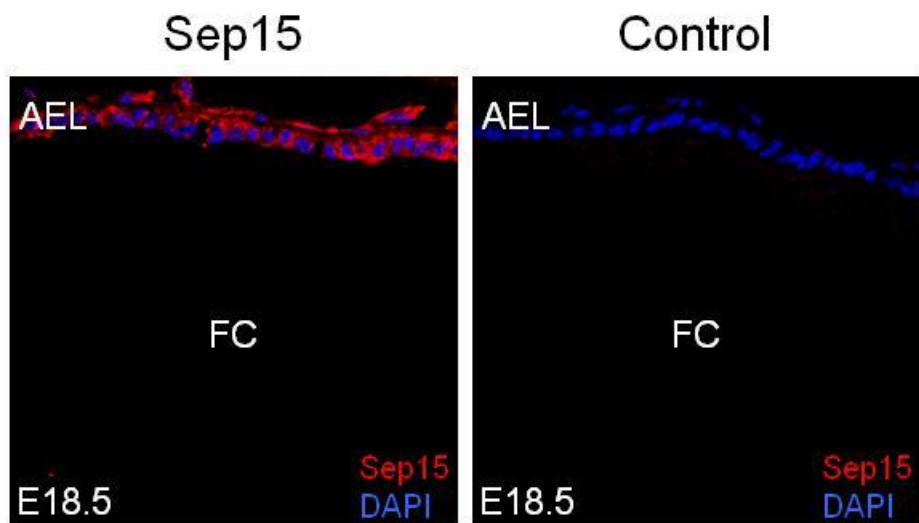


**Figure S4. Sep15 expression in the lens during development.** Mouse embryonic coronal section at E18.5 was stained with Sep15 antibody (Sep15) or with secondary antibody-only as a negative control (Control). AEL, anterior epithelium of the lens. FC, fiber cells. Sep15 staining is in red, and DAPI in blue.

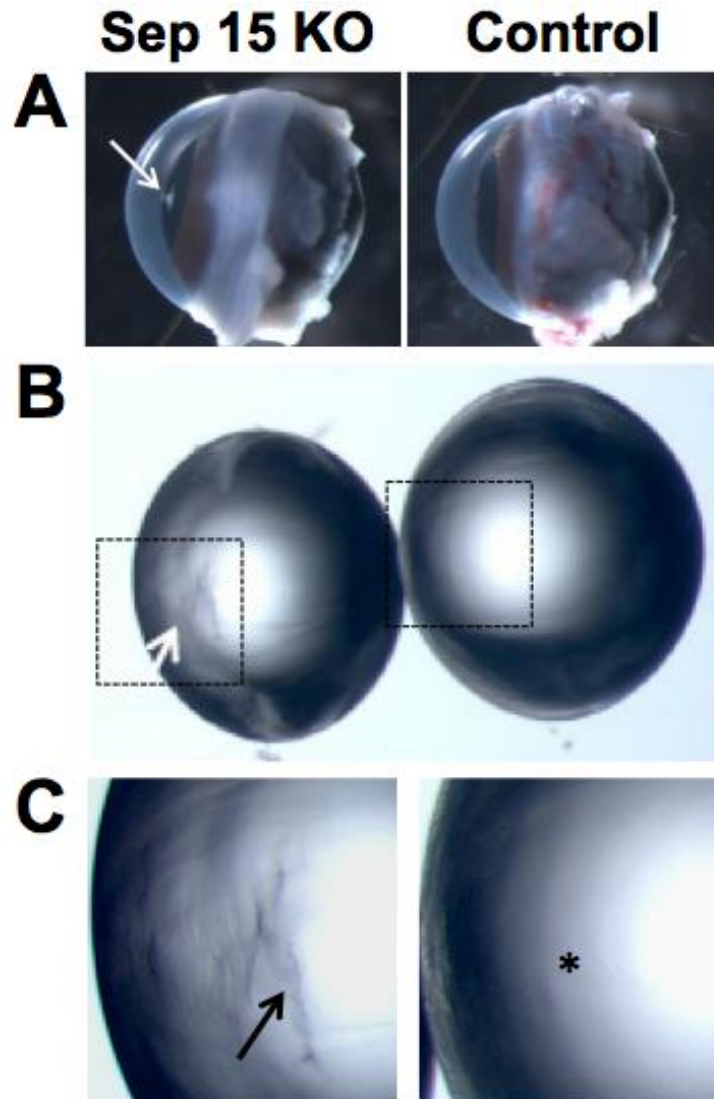


**Figure S5. Development of cataracts in Sep15 KO mice.** (A) Whole eyeball dissected from a 10-month old Sep15 KO female, which had anterior nuclear cataract (white arrow). Lenses of WT mice were clear, while opacity was evident in Sep15 KO mice. (B) Lenses dissected from a 10-month old Sep15 KO and WT (control) male mice. (C) High magnification images from boxed region in (B). Arrows in B and C point to the detected abnormalities. Absence of abnormalities (asterisk) in the control lenses.

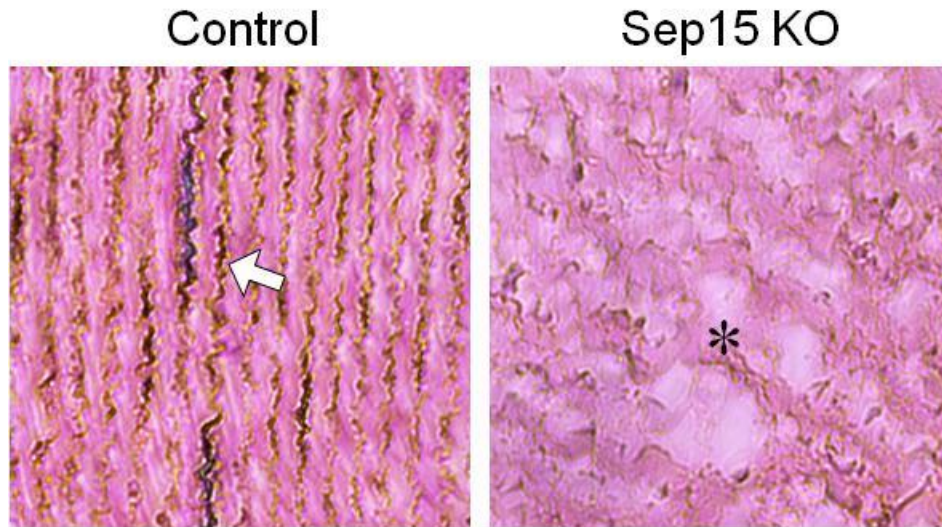


**Figure S6. Histological analysis of control and Sep15 KO mice.** H&E staining of lens sections from 3 month old WT and Sep15 KO mice is shown. At 40x magnification, abnormalities in the central region of the lens can be detected in Sep15 KO mice, but not in control. White arrow indicates the regular pattern of lens fiber cells in control lens, and asterisk shows disruption of this structure in the Sep15 KO lens.

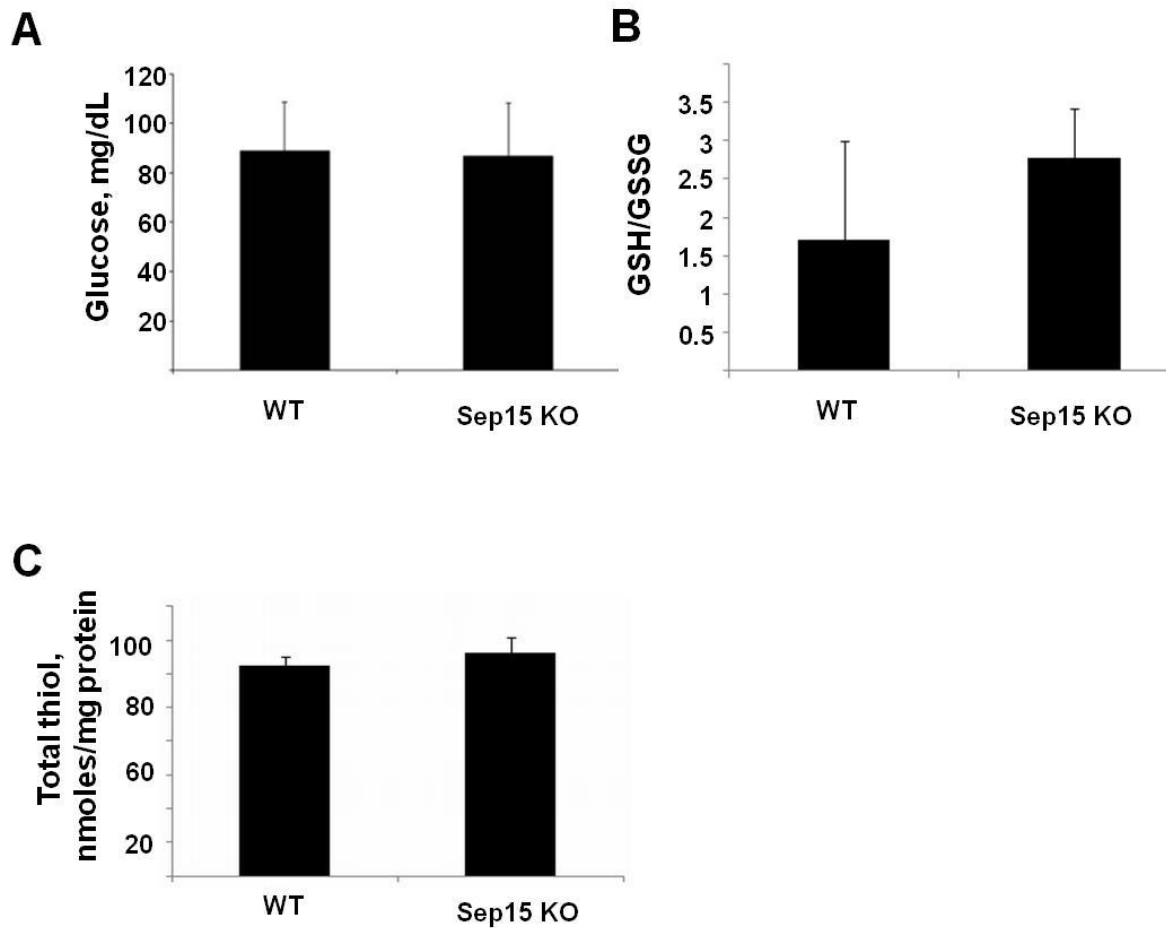


**Figure S7. Comparison of glucose levels and oxidative stress parameters in the lenses of WT and Sep15 KO mice.** (A) WT and Sep15 KO mice were fasted overnight and blood was analyzed for glucose levels (n=9 for WT and 12 for Sep15 KO mice). (B) Lenses were extracted from WT and Sep15 KO mice. Protein extracts were analyzed for (B) ratio of oxidized to reduced glutathione and (C) total thiol levels. In each group, n=3.